Ceramides Dissociate Steatosis and Insulin Resistance in the Human Liver in Non-Alcoholic Fatty Liver Disease

Short title: Ceramides in Human Non-Alcoholic Fatty Liver Disease

Panu K. Luukkonen[1, 2*], You Zhou[1*], Sanja Sädevirta[1, 2], Marja Leivonen[3], Johanna Arola[4], Matej Orešič[5], Tuulia Hyötyläinen[5], Hannele Yki-Järvinen[1, 2]

[1]Minerva Foundation Institute for Medical Research, Helsinki, Finland, [2]Department of Medicine, [3]Department of Surgery and [4]Department of Pathology, University of Helsinki and Helsinki University Hospital, Helsinki, Finland, [5]Steno Diabetes Center, Gentofte, Denmark

These authors contributed equally to this work

GRANT SUPPORT: This study was supported by research grants from the Academy of Finland (HY), EU/EFPIA Innovative Medicines Initiative Joint Undertaking (EMIF grant no. 115372, HY), the Sigrid Juselius (HY), EVO (HY) and the Novo Nordisk (HY) Foundations. The authors are members of the EPoS (Elucidating Pathways of Steatohepatitis) consortium funded by the Horizon 2020 Framework Program of the European Union under Grant Agreement 634413.

ABBREVIATIONS:

ALP	alkaline phosphatase
ALT	alanine aminotransferase
AST	aspartate aminotransferase
BMI	body mass index
CoA	coenzyme A
DAG	diacylglycerol
DNL	*de novo* lipogenesis
FFA	free fatty acid
GGT	gamma-glutamyl transferase
HDL	high density lipoprotein
HOMA-IR	homeostasis model assessment of insulin resistance
IR	insulin resistance
NAFLD	non-alcoholic fatty liver disease
NASH	non-alcoholic steatohepatitis
OGTT	oral glucose tolerance test
PNPLA3	patatin-like phospholipase domain containing protein 3
TAG	triacylglycerol

CORRESPONDING AUTHOR:

Panu K. Luukkonen, MD,

Tukholmankatu 8

00290 Helsinki

FINLAND

E-mail: panu.luukkonen@fimnet.fi

Phone: +358 294125708

DISCLOSURES: None.

ELECTRONIC WORD COUNT: 5989 words.

FIGURES: 5

TABLES: 1

AUTHOR CONTRIBUTIONS: PL – study concept and design; acquisition of data; analysis and interpretation of data; drafting of the manuscript; critical revision of the manuscript for important intellectual content; statistical analysis. YZ – study concept and design; analysis and interpretation of data; drafting of the manuscript; critical revision of the manuscript for important intellectual content; statistical analysis. SS, ML, JA, MO, TH – acquisition of data; critical revision of the manuscript for important intellectual content. HY – study concept and design; analysis and interpretation of data; drafting of the manuscript; critical revision of the manuscript for important intellectual content; obtained funding; study supervision.

ABSTRACT:

Background and Aims: Recent data in mice have identified *de novo* ceramide synthesis as the key mediator of hepatic insulin resistance (IR) that in humans characterizes increases in liver fat due to IR ('Metabolic NAFLD' but not that due to the I148M gene variant in PNPLA3 ('PNPLA3 NAFLD'). We determined which bioactive lipids co-segregate with IR in the human liver.

Methods: Liver lipidome was profiled in liver biopsies from 125 subjects that were divided into equally sized groups based on median HOMA-IR ('High and Low HOMA-IR', n=62 and n=63) or PNPLA3 genotype ($PNPLA3^{148MM/MI}$, n=61 vs. $PNPLA3^{148II}$, n=64). The subjects were also divided into 4 groups who had either IR, the I148M gene variant, both of the risk factors or neither.

Results: Steatosis and NASH prevalence were similarly increased in 'High HOMA-IR' and $PNPLA3^{148MM/MI}$ groups compared to their respective control groups. The 'High HOMA-IR' but not the $PNPLA3^{148MM/MI}$ group had features of IR. The liver in 'High HOMA-IR' vs. 'Low HOMA-IR' was markedly enriched in saturated and monounsaturated triacylglycerols and free fatty acids, dihydroceramides (markers of *de novo* ceramide synthesis) and ceramides. Markers of other ceramide synthetic pathways were unchanged. In $PNPLA3^{148MM/MI}$ vs. $PNPLA3^{148II}$, the increase in liver fat was due to polyunsaturated triacylglycerols while other lipids were unchanged. Similar changes were observed when data were analyzed using the 4 subgroups.

Conclusions: Similar increases in liver fat and NASH are associated with a metabolically harmful saturated, ceramide-enriched liver lipidome in 'Metabolic NAFLD' but not in 'PNPLA3 NAFLD'. This difference may explain why metabolic but not PNPLA3 NAFLD increases the risk of type 2 diabetes and CVD.

KEYWORDS: Patatin-like phospholipase domain containing protein 3

Introduction

Both features of the metabolic syndrome and non-alcoholic fatty liver disease (NAFLD) predict type 2 diabetes and cardiovascular disease even independent of obesity in several prospective studies [1]. Such a form of NAFLD ('Metabolic NAFLD') is characterized by hepatic insulin resistance (IR) [2,3], increased serum triacylglycerols (TAG), low HDL cholesterol and low serum adiponectin concentrations [4]. The latter may reflect adipose tissue inflammation [5,6]. 'Metabolic NAFLD' precedes and predicts type 2 diabetes and CVD [1].

In insulin-resistant 'Metabolic NAFLD', studies tracing pathways contributing to intrahepatocellular TAGs have shown that increased hepatic *de novo* lipogenesis (DNL) is the major cause for increased intrahepatocellular TAG content in 'Metabolic NAFLD'[7]. DNL produces exclusively saturated fatty acids, which can be desaturated to form monounsaturated fatty acids by SCD-1 [8,9]. A hepatic venous catheterization study showed that fatty liver overproduces saturated TAGs [10].

At least two classes of bioactive lipids, ceramides and diacylglycerols (DAGs), have been suggested to mediate insulin resistance. The 'ceramide-centric' view postulates both saturated fat from DNL or from the diet and adiponectin deficiency induce IR via increasing ceramide synthesis [11]. Ceramides also induce ER stress and mitochondrial dysfunction, which characterize human NAFLD [12]. The immediate precursors of TAGs, DAGs induce IR by inhibiting PI3-kinase and Akt/protein kinase B activation via stimulation of protein kinase C isoforms [13].

Ceramides can be synthesized via the *de novo* synthetic pathway from palmitate, via

sphingomyelin hydrolysis and via the salvage pathway, which uses hexosylceramides as its substrate [11]. Two very recent studies in mice identified the same sphingolipid species, C16:0-ceramide, formed via ceramide synthase 6, in the *de novo* ceramide synthetic pathway as the principal mediator of obesity-related insulin resistance [14-16]. There are no human data to examine which if any of these pathways contributes to changes in ceramide concentrations in the human liver.

A common I148M variant in PNPLA3 at rs738409 increases liver fat content [17]. Depending on ethnicity, 20-50% of all subjects carry this gene variant [17]. *In vitro*, this gene variant inhibits lipolysis of TAGs in the liver [18] and acts as a gain-of-function mutation to increase TAG synthesis by acting as a lysophosphatidic acyltransferase (LPAAT) converting lysophosphatidic acid into phosphatitidic acid [19]. Monounsaturated fatty acid containing acyl CoAs such as oleyl CoA are preferred substrates for the former activity while polyunsaturated fatty acyl CoAs such as linoleoyl and arachidonoyl CoA are preferred substrates for the latter activity [18,19]. In contrast to the metabolic abnormalities observed in 'Metabolic NAFLD', NAFLD due to the I148M variant ('PNPLA3 NAFLD') is not characterized by features of insulin resistance such as adipose tissue inflammation, adiponectin deficiency or an increased risk of type 2 diabetes and CVD [20,21].

'Metabolic NAFLD' and 'PNPLA3 NAFLD' provide models to characterize how insulin resistance and steatosis dissociate in the human liver. Given the high prevalence of both the metabolic syndrome and the I148M PNPLA3 gene variant, some individuals will have both of these risk factors for NAFLD. In the present study, we hypothesized that the liver in 'Metabolic NAFLD' might be characterized by

increased concentrations of saturated/monounsaturated TAGs, free fatty acids (FFA) and IR-inducing bioactive lipids, while such metabolically harmful lipids may not be found in 'PNPLA3 NAFLD'. To this end, we analyzed the human liver lipidome in 125 liver biopsy samples using ultra high performance liquid chromatography (UHPLC) and gas chromatography combined with mass spectrometry (MS). This was done in groups divided based on median HOMA-IR into those with 'High HOMA-IR' (a model for 'Metabolic NAFLD') and 'Low HOMA-IR', and based on genotyping at rs738409 into carriers ($PNPLA3^{148MM/MI}$) (a model for 'PNPLA3 NAFLD') and non-carriers ($PNPLA3^{148II}$) of the PNPLA3 I148M gene variant. We also compared liver lipidomes in 4 groups of subjects who had both IR and carried the I148M gene variant ('double trouble'), either ('single trouble') or neither risk factor.

Materials and methods

Study subjects

A total of 125 subjects were recruited amongst those undergoing laparoscopic bariatric surgery. Subjects were eligible if they met the following criteria: (a) age 18 to 75 years; (b) no known acute or chronic disease except for obesity or type 2 diabetes or hypertension on the basis of medical history, physical examination and standard laboratory tests (complete blood count, serum creatinine, electrolyte concentrations); (c) alcohol consumption less than 20 g per day for women and less than 30 g per day for men; (d) no clinical or biochemical evidence of other liver disease, or clinical signs or symptoms of inborn errors of metabolism; (e) no history of use of toxins or drugs associated with liver steatosis. Elevated liver enzymes (ALT and AST) were not exclusion criteria. The study protocol was approved by the ethics committee of the Hospital District of Helsinki and Uusimaa. The study was conducted in accordance with the Declaration of Helsinki. Each participant provided written informed consent after being explained the nature and potential risks of the study.

Metabolic study

The subjects were invited to a separate clinical visit one week prior to surgery for detailed metabolic characterization. The subjects came to the clinical research center after an overnight fast. Body weight, height and waist circumference were measured as described [21]. An intravenous cannula was inserted in the antecubital vein for withdrawal of blood for measurement of HbA_{1c}, serum insulin and adiponectin, plasma glucose, LDL- and HDL-cholesterol, triglyceride, albumin, AST, ALT, ALP and GGT concentrations and for genotyping as described [21]. Plasma albumin was measured using a photometric method on an autoanalyzer (Modular Analytics EVO;

Hitachi High-Technologies Corporation, Tokyo, Japan). PNPLA3 at rs739409 was genotyped as previously described [22]. After basal blood sampling and anthropometric measurements, an oral glucose (75 grams) tolerance test (OGTT) was performed [23]. Homeostasis model assessment of insulin resistance (HOMA-IR) was used as a proxy for IR by using the formula: HOMA-IR = fS-insulin (mU/l) x fP-glucose (mmol/l) / 22.5 [24]. Matsuda insulin sensitivity index was used as another measure of insulin sensitivity. This measure was calculated from insulin and glucose concentrations measured at 0, 30 and 120 minutes during the OGTT [25]. Body weight of the subjects was similar at the time of the metabolic study and surgery (131.1±2.0 and 130.1±2.1 kg, NS).

The subjects (n=125) were divided into two groups based on insulin resistance, as defined by median HOMA-IR. Because of lack of universally accepted consensus regarding the cut-off threshold of HOMA-IR between the insulin-resistant and sensitive subjects, median HOMA-IR was used to divide the subjects into 'High HOMA-IR' (HOMA-IR > 3.19) and 'Low HOMA-IR' (HOMA-IR ≤ 3.19) groups. In retrospect, this cut-off was very similar to the HOMA-IR cut-off differentiating subjects with and without NASH (3.38) (see Supplementary Material). However, as the primary aim was to examine how risk factors (IR or the PNPLA3 gene variant) influenced the liver lipidome as well as other features including liver histology, we did not a priori divide the subjects into groups based on NASH.

Since some patients are both insulin resistant and carry the PNPLA3 gene variant, we also divided the subjects 2x2 based on both of these characteristics into 4 groups

(Venn diagram as Supplementary Fig. 1 and other data as Supplementary Material p. 11-13, Supplementary Figures 6-8 and Supplementary Table 2).

Liver biopsies and liver histology

Immediately at the beginning of the surgery, wedge biopsies of the liver were obtained. Part of the biopsy was sent to the pathologist for histological assessment, and the rest was snap-frozen in liquid nitrogen for subsequent analysis of molecular lipids. The time from obtaining the biopsy until freezing the sample in liquid nitrogen was approximately one minute. Liver histology was analyzed by an experienced liver pathologist (J.A.) in a blinded fashion as proposed by Brunt et al [26].

Lipidomic analysis

The lipidome was analyzed using UHPLC-MS as described in Supplementary Material. The analyses covered most of the main molecular lipids, including ceramides, dihydroceramides, TAGs, DAGs, sphingomyelins, hexosylceramides, phosphatidylcholines (PC), phosphatidylethanolamines (PE), phosphatidylserines (PS), and lysophosphosphatidylcholines. The lipid identification was based on an internal library, which had been constructed based on accurate mass measurements in combination with tandem mass measurements. For specific lipids, the composition of fatty acid chains had been determined with separate measurements, and for those the fatty acid composition was specified, e.g. TAG(14:0/16:0/18:0).

Cluster analysis of lipids

We performed Bayesian model-based clustering analysis to identify the groups of lipids with similar profiles across all the samples as described in the Supplementary Material.

Analysis of pathways of ceramide synthesis

The first step of the *de novo* ceramide synthetic pathway converts palmitate and serine to 3-ketosphinganine and ultimately to dihydroceramides prior to formation of ceramides (Fig. 5). The sphingomyelin hydrolysis pathway results in formation of ceramides via hydrolysis of sphingomyelins. The salvage pathway generates ceramides by breakdown of complex sphingolipids, such as hexosylceramides (Fig. 5) [11]. In the present study, we analyzed the concentrations of dihydroceramides, sphingomyelins and hexosylceramides as markers of these pathways, respectively.

Analysis of hepatic free fatty acids

The free fatty acid analyses were performed using GC-MS as described in the Supplementary Material.

Statistical analyses

Continuous variables were tested for normality using the Kolmogorov-Smirnov test. The independent two-sample Student *t* test and Mann-Whitney *U* test were used to compare normally and non-normally distributed data, respectively. Normally distributed data were reported in means ± standard error of means while non-normally distributed were reported in medians and interquartile ranges. Pearson's $\chi 2$ test was used to evaluate if the distribution of categorical variables differ between the groups. Statistical analyses were performed by using R 3.1.1 (http://www.r-project.org/), IBM SPSS Statistics 22.0.0.0 version (IBM, Armonk, NY) and GraphPad Prism 6.0f for Mac OS X (GraphPad Software, La Jolla, CA). A two-sided *p*-value of less than 0.05 indicated statistical significance.

Results

Characteristics of the study groups

Characteristics of the HOMA-IR and PNPLA3 genotype subgroups are shown in Table 1. All groups were similar with respect to gender (Table 1) and BMI (Fig. 1).

HOMA-IR subgroups

Liver fat was significantly and 3-fold higher in the 'High HOMA-IR' (15 [5–33]) than in the 'Low HOMA-IR' group (5 [0–20], $p<0.002$, Fig. 1A). The 'High HOMA-IR' group had significantly higher fasting serum insulin concentrations than the 'Low HOMA-IR' group (Fig. 1A) and also higher glucose and insulin concentrations in the OGTT (Fig. 1B).

The 'High HOMA-IR' group had higher triglyceride and lower HDL cholesterol and adiponectin concentrations compared to the 'Low HOMA-IR' group (Table 1 and Fig. 1A). The prevalence of NASH was significantly increased in the 'High HOMA-IR' as compared to the 'Low HOMA-IR' group (Table 1). The distributions of PNPLA3 genotypes were similar in 'High HOMA-IR' and 'Low HOMA-IR' (Table 1).

Subgroups based on PNPLA3 genotype

Liver fat was significantly and 3-fold higher in the 'PNPLA3$^{148MM/MI}$' (15 [5–30]) than the 'PNPLA3^{148II}' group (5 [0–28], $p<0.04$, Fig. 1A). Glucose and insulin concentrations, HOMA-IR, serum lipid and adiponectin concentrations were similar between the subgroups (Table 1 and Fig. 1A). The prevalence of NASH was significantly increased in the PNPLA3$^{148MM/MI}$ as compared to the PNPLA3^{148II} group.

Liver TAGs

Saturated and monounsaturated TAGs were particularly enriched in 'High HOMA-IR' as compared to the 'Low HOMA-IR' group. In contrast, these TAGs were similar between PNPLA3 subgroups (Fig. 2). The PNPLA3$^{148MM/MI}$ compared to the PNPLA3^{148II} group displayed significant increases in polyunsaturated TAGs containing 3 to 11 double bonds (Fig. 2). Similar differences in TAGs between PNPLA3 subgroups were observed when this analysis was performed in 'Low HOMA-IR' subjects alone (Supplementary Fig. 3). The number of double bonds in TAGs was inversely related to relative TAG concentrations between the 'High' as compared to 'Low HOMA-IR' group, but positively related between the PNPLA3 subgroups (Supplementary Fig. 4).

Liver FFAs

Hepatic concentrations of free palmitate (C16:0) (372 [296–502] vs 333 [279–402] nmol/g, $p<0.05$), stearate (C18:0) (202 [149–250] vs 164 [135–200], $p<0.05$) and oleate (C18:1) (188 [140–254] vs 164 [126– 207], $p<0.05$) were significantly higher in the 'High HOMA-IR' than the 'Low HOMA-IR' group. The polyunsaturated free linoleate (C18:2) and arachidonate (C20:4) were similar between the HOMA-IR subgroups (Fig. 3). Hepatic FFAs did not differ between the 'PNPLA3^{148II}' and 'PNPLA3$^{148MM/MI}$' groups (Fig. 3).

Liver ceramides

Ceramide concentrations. Almost all ceramide species were significantly increased in the 'High HOMA-IR' as compared to the 'Low HOMA-IR' group while there were no change between the PNPLA3$^{148MM/MI}$ and PNPLA3^{148II} groups (Fig. 4). This was also true when the PNPLA3 subgroups were compared within the 'Low HOMA-IR' group (Supplementary Fig. 3).

Pathways of ceramide synthesis. The hepatic concentrations of dihydroceramides (markers of *de novo* synthesis), sphingomyelins (markers of sphingomyelin hydrolysis) and hexosylceramides (markers of the salvage pathway) were analysed to determine which ceramide synthetic pathway was upregulated in the 'High HOMA-IR' as compared to the 'Low HOMA-IR' group. Concentrations of 4 out of 5 dihydroceramide species were significantly increased in 'High' as compared to 'Low HOMA-IR' group, while the concentrations of sphingomyelins and hexocylceramides were unchanged (Fig. 5). In all subjects, there was an inverse relationship between serum adiponectin and total hepatic ceramides ($r = -0.21$, $p = 0.022$).

Liver DAGs

Four DAG species were significantly increased in the 'High' vs. the 'Low HOMA-IR' group, and one polyunsaturated species between the PNPLA3$^{148MM/MI}$ vs. the PNPLA3^{148II} group (Supplementary Fig. 5).

Paired analyses of HOMA-IR and PNPLA3 with 4 groups

Subject characteristics of the 4 subgroups (High HOMA-IR and variant carrier i.e. $PNPLA3^{148MM/MI}$, Low HOMA-IR and variant, High HOMA-IR and no variant, Low HOMA-IR and no variant) are shown in Supplementary Table 2, Supplementary Fig. 6-8 and on page 11-13 of the Supplement.

Insulin resistance (comparison of High HOMA-IR and Low HOMA-IR in subjects carrying the I148M gene variant) increased TAGs with no or few double bonds while the PNPLA3 gene variant (comparison of variant allele carriers and no carriers in subjects with similar HOMA-IR) increased polyunsaturated TAGs (Supplementary Fig. 7). Insulin resistance also increased almost all ceramides in the face of a similar genetic background while the I148M gene variant had no effect on ceramides in the face of similar HOMA-IR (Supplementary Fig. 8).

Discussion

In the present study, we analyzed the human liver lipidome in two types of NAFLD, one defined based on IR ('Metabolic NAFLD') and the other based on PNPLA3 genotype at rs738409 ('PNPLA3 NAFLD'). Both types of NAFLD had a similar increase in % liver fat and NASH. The liver lipidome in 'Metabolic NAFLD' was characterized by an increase in saturated and monounsaturated TAGs and FFA while the liver in 'PNPLA3 NAFLD' predominantly contained an excess of polyunsaturated TAGs with no changes in FFA. The liver in 'Metabolic NAFLD' but not 'PNPLA3 NAFLD' was markedly enriched in insulin-resistance inducing ceramides synthesized via the *de novo* ceramide synthetic pathway (Fig. 4).

To define 'Metabolic NAFLD', we divided the subjects based on median HOMA-IR. We and others have previously performed direct measurements of insulin sensitivity and shown that fasting insulin concentrations as well as directly measured hepatic insulin sensitivity correlate with liver fat content [3,27]. There are no universally accepted criteria for IR using HOMA-IR. Since we wanted to examine how the etiology (insulin resistance or the PNPLA3 I148M variant or both) influences the liver lipidome and histology rather than vice versa, we divided the subjects based on these characteristics rather than histology. The median HOMA-IR (3.2), was comparable to the HOMA-IR value differentiating subjects with and without NASH (3.4). The use of median HOMA-IR also resulted in subgroups with an almost identical sample size, age, gender, BMI and similar increases in liver fat and NASH prevalence, thus enabling examination of effects of IR and effects of the PNPLA3 I148M gene variant on liver lipidome independently of confounders. To further dissect effects of insulin resistance and the gene variant on the liver lipidome, we also compared PNPLA3 subgroups within the 'Low HOMA-IR' group (Fig. 3) and performed a 2x2 analysis

where the subjects were grouped into those with ‘double trouble’ (both PNPLA3 I148M gene variant and insulin resistance), ‘single trouble’ (either gene variant or insulin resistance), or neither. These additional analyses yielded results similar to those of grouping all subjects either based on the gene variant or HOMA-IR (Table 1, Fig. 1-4, Supplementary Table 2, Supplementary Fig. 6-8).

The PNPLA3 variant allele carriers as compared to the non-carriers had a significantly higher liver fat content and no features of insulin resistance as determined from HOMA-IR, serum lipids and adiponectin concentrations. Lack of IR was also verified by calculating the Matsuda index from glucose and insulin concentrations measured during the OGTT (Table 1) and is consistent with 13 out of 15 previous studies showing no increased insulin resistance in ’PNPLA3 NAFLD’ [21]. Our study cohort included 66 % women and 34 % men, which is not representative of epidemiologic studies, in which NAFLD is more prevalent in men than in women [28]. However, the gender distributions were comparable between all subgroups, and also in subjects with NASH.

The liver biopsies were taken after an overnight fast, when peripheral lipolysis and DNL are the main sources of fatty acids for synthesis of triacylglycerols in the liver [29]. Although there are no previous studies comparing the liver lipidome in NAFLD defined by HOMA-IR, the increase in the saturated and monounsaturated TAG species is consistent with previous data in common NAFLD. Lambert et al showed in groups of 13 subjects with a high and 13 subjects with a low liver fat content using multiple stable isotopes that DNL was 3-fold increased in subjects with high vs. low liver fat content [7]. DNL produces exclusively saturated fatty acids from substrates such as amino acids and simple sugars [29]. The other pathway that provides fatty

acids for intrahepatocellular triglycerols in NAFLD is adipose tissue lipolysis [30-32]. The increase in free saturated and monounsaturated fatty acids in the 'High HOMA-IR' vs. the 'Low HOMA-IR' group could reflect either lipolysis or DNL. Since the human liver contains 2-fold more stearate (C18:0) and also significantly more palmitate (C16:0) than subcutaneous and intra-abdominal adipose tissue [33], the increase in saturated fatty acids likely predominantly reflects DNL.

Of two major classes of bioactive lipids capable of inducing insulin resistance, we found virtually all ceramides to be significantly increased in 'Metabolic NAFLD' (Fig. 4). In keeping with the increase in free palmitate (C16:0), the *de novo* ceramide synthetic pathway, as determined from the dihydroceramide concentrations, but not other ceramide synthetic pathways, was increased (Fig. 5). Formation of dihydroceramides is catalyzed by six different ceramide synthases (CerS1-6). *CerS6* deficient mice exhibit reduced C16:0-ceramides such as Cer(d18:1/16:0) and are protected from high fat induced obesity, insulin resistance and adipose tissue inflammation [15]. A complementary paper showed that heterozygous *CerS2* knockout mice, which are characterized by upregulation of C16:0-ceramides, display increased liver triglyceride and macrophage content, glucose intolerance and hyperinsulinemia [16]. The increases in the 16:0 and 18:0 dihydroceramides in the insulin-resistant human liver (Fig. 5) are entirely consistent with these recent mouse data.

Adiponectin regulates ceramide metabolism by upregulating ceramidase, the enzyme which which degrades ceramide to sphingosine [11]. Thus, adiponectin deficiency contributes to increased ceramide concentrations via impaired degradation. In the present study, the 'High HOMA-IR' group had lower serum adiponectin concetrations

than the 'Low HOMA-IR' group and there was a weak inverse correlation between serum adiponectin concentrations and ceramides in the liver. Adiponectin concentrations were similar in subjects with and without PNPLA3 I148M variant.

Total hepatic DAGs have been previously shown to correlate with liver fat and fasting insulin/HOMA-IR in groups of 16 [9], 16 [34] and 37 [35] subjects. In the present study, 4 out of 5 DAGs, which are immediate precursors of TAGs, were increased in the 'Metabolic NAFLD'. One DAG species was increased in the 'PNPLA3 NAFLD'. The number of DAGs identified was low compared to the number of ceramides (Fig. 4 vs. Supplementary Fig. 6) and it was not feasible to measure DAGs separately in subcellular compartments. Thus, the present data do not exclude the possibility that DAGs contribute to IR in the human liver. Along the same lines, even though the lipidome analyzed in the present study is the largest hitherto performed, there are other lipids which were not analyzed by the current platforms such as lysophosphatidic acid, phosphatidic acid, eicosanoids and endocannabinoids which may act as second messengers on key metabolic pathways [36].

Liver polyunsaturated TAGs were strikingly different between PNPLA3 variant allele carriers and non-carriers (Fig. 2). Kumari et al showed that human recombinant PNPLA3 I148M increases LPAAT activity from long unsaturated fatty acid containing CoAs such as arachnidonoyl and linoleoyl CoA much more than from saturated CoA [19]. The increase in polyunsaturated TAGs in the present study in the I148M variant allele carriers is thus compatible with these gain-of-function data as the increased TAGs in the 'PNPLA3 NAFLD' were long and highly unsaturated. The fold-increase in TAGs was particularly apparent in TAGs containing 5-8 double bonds (Fig. 2 and Supplementary Fig. 4). The increase in polyunsaturated DAGs in

the 'PNPLA3 NAFLD' is also compatible with the gain-of-function data. The lack of change in hepatic FFAs, which covered 80% of previously described all human liver FFAs and 87% of all free polyunsaturated fatty acids [37], supports the idea that the increase in polyunsaturated hepatic TAGs in 'PNPLA3 NAFLD' was driven by increased enzymatic activity rather than substrate availability.

Few differences were observed in concentrations of saturated and monounsaturated TAGs between the PNPLA3 subgroups. In addition to LPAAT activity, the gene variant also inhibits lipolysis of TAGs containing especially monounsaturated fatty acids when overexpressed in the mouse liver [18]. This mechanism does not seem to explain the present data although it could have contributed to increases in monounsaturated fatty acids in the polyunsaturated TAGs.

We are aware of one previous study, which characterized relative fatty acid profiles using thin layer chromatography between 19 subjects carrying the I148M variant allele carriers and 33 non-carriers undergoing liver surgery [38]. A relative reduction in stearic acid was found in keeping with the present data. However, the subjects were not characterized or analyzed with respect to features of insulin resistance or ceramides and TAGs by chain length and number.

The subjects with 'Metabolic NAFLD' and 'PNPLA3 NAFLD' had an equal frequency of NASH (Table 1) despite very different hepatic triglyceride and bioactive lipid compositions. Previous studies have clearly established that the PNPLA3 gene variant prediposes to NASH independent of features insulin resistance [39]. Several possible mechanisms could increase the risk of NASH in carriers of the I148M gene

variant. PUFAs, once in TAGs, are metabolically inert and as such cannot contribute to NASH [40]. In the present study, which included measurement of liver FFA, the concentration of free unsaturated fatty acids were unchanged in PNPLA3 I148M variant allele carriers compared to non-carriers. We therefore cannot ascribe changes in liver histology to those in polyunsaturated fatty acids. Simple steatosis without hepatocellular injury has been recently shown to predict NASH [41]. In NASH, fat accumulates in the perivenous area in Zone 3 [26], which is characterized by impaired microcirculation and decreased oxygen concentrations [42]. Ballooning necrosis occurs in the midst of such fat-filled regions [26]. The PNPLA3 gene variant could therefore simply increase the risk of NAFLD by increasing steatosis. Histologically, PNPLA3 variant allele carriers have all features of NASH [43]. The PNPLA3 gene variant may also have effects outside hepatocytes in stellate cells [44] and extrahepatic tissues [45].

In conclusion, the present data show that insulin resistance in the human liver is associated with increased concentrations of saturated and monounsaturated FFAs and TAGs as well as ceramides from the *de novo* ceramide synthetic pathway. These data are consistent with several known pathophysiologic features of human 'Metabolic NAFLD'. The human liver lipidome in 'PNPLA3 NAFLD' lacks all of these changes and is characterized by increased concentrations of polyunsaturated TAGs, which can be attributed to known functions of the I148M variant in *in vitro* studies [18,19]. Both types of NAFLD confer increased prevalence of NASH suggesting that increased concentrations of bioactive lipids are not necessary for development of NASH.

Acknowledgements

We acknowledge Marju Orho-Melander, Janne Makkonen, Ksenia Sevastianova, Alexandre Santos, and Jukka Westerbacka for their contributions and the volunteers for their help. We thank Anne Salo, Aila Karioja-Kallio, Mia Urjansson, Katja Sohlo, Erja Juvonen, Anna-Liisa Ruskeepää, Ulla Lahtinen, Heli Nygren and Ismo Mattila for their excellent technical assistance.

References

[1] Anstee QM, Day CP. The genetics of NAFLD. Nat Rev Gastroenterol Hepatol. 2013;10:645–55.

[2] Ryysy L, Häkkinen AM, Goto T, Vehkavaara S, Westerbacka J, Halavaara J, et al. Hepatic fat content and insulin action on free fatty acids and glucose metabolism rather than insulin absorption are associated with insulin requirements during insulin therapy in type 2 diabetic patients. Diabetes 2000;49:749–58.

[3] Seppälä-Lindroos A, Vehkavaara S, Häkkinen A-M, Goto T, Westerbacka J, Sovijärvi A, et al. Fat accumulation in the liver is associated with defects in insulin suppression of glucose production and serum free fatty acids independent of obesity in normal men. J Clin Endocrinol Metab 2002;87:3023–8.

[4] Turer AT, Browning JD, Ayers CR, Das SR, Khera A, Vega GL, et al. Adiponectin as an independent predictor of the presence and degree of hepatic steatosis in the Dallas Heart Study. J Clin Endocrinol Metab 2012;97:E982–6.

[5] Kolak M, Westerbacka J, Velagapudi VR, Wågsäter D, Yetukuri L, Makkonen J, et al. Adipose tissue inflammation and increased ceramide content characterize subjects with high liver fat content independent of obesity. Diabetes 2007;56:1960–8.

[6] Tordjman J, Poitou C, Hugol D, Bouillot J-L, Basdevant A, Bedossa P, et al. Association between omental adipose tissue macrophages and liver histopathology in morbid obesity: Influence of glycemic status. J Hepatol 2009;51:354–62.

[7] Lambert JE, Ramos-Roman MA, Browning JD, Parks EJ. Increased de novo lipogenesis is a distinct characteristic of individuals with nonalcoholic fatty liver disease. Gastroenterology 2014;146:726–35.

[8] Aarsland A, Wolfe RR. Hepatic secretion of VLDL fatty acids during stimulated lipogenesis in men. J. Lipid Res. 1998;39:1280–1286.

[9] Kotronen A, Seppänen-Laakso T, Westerbacka J, Kiviluoto T, Arola J, Ruskeepää A-L, et al. Hepatic stearoyl-CoA desaturase (SCD)-1 activity and diacylglycerol but not ceramide concentrations are increased in the nonalcoholic human fatty liver. Diabetes. 2009;58:203–208.

[10] Westerbacka J, Kotronen A, Fielding BA, Wahren J, Hodson L, Perttilä J, et al. Splanchnic balance of free fatty acids, endocannabinoids, and lipids in subjects with nonalcoholic fatty liver disease. Gastroenterology. 2010;139:1961–1971.

[11] Chavez JA, Summers SA. A ceramide-centric view of insulin resistance. Cell Metab. 2012;15:585–594.

[12] Koliaki C, Roden M. Hepatic energy metabolism in human diabetes mellitus, obesity and non-alcoholic fatty liver disease. Mol. Cell. Endocrinol. 2013;379:35–42.

[13] Perry RJ, Samuel VT, Petersen KF, Shulman GI. The role of hepatic lipids in hepatic insulin resistance and type 2 diabetes. Nature. 2014;510:84–91.

[14] Hla T, Kolesnick R. C16:0-ceramide signals insulin resistance. Cell Metab. 2014;20:703–705.

[15] Turpin SM, Nicholls HT, Willmes DM, Mourier A, Brodesser S, Wunderlich CM, et al. Obesity-induced CerS6-dependent C16:0 ceramide production promotes weight gain and glucose intolerance. Cell Metab. 2014;20:678–686.

[16] Raichur S, Wang ST, Chan PW, Li Y, Ching J, Chaurasia B, et al. CerS2 haploinsufficiency inhibits β-oxidation and confers susceptibility to diet-induced steatohepatitis and insulin resistance. Cell Metab. 2014;20:687–695.

[17] Romeo S, Kozlitina J, Xing C, Pertsemlidis A, Cox D, Pennacchio LA, et al. Genetic variation in PNPLA3 confers susceptibility to nonalcoholic fatty liver disease. Nat Genet 2008;40:1461–5.

[18] Huang Y, Cohen JC, Hobbs HH. Expression and characterization of a PNPLA3 protein isoform (I148M) associated with nonalcoholic fatty liver disease. J. Biol. Chem. 2011;286:37085–37093.

[19] Kumari M, Schoiswohl G, Chitraju C, Paar M, Cornaciu I, Rangrez AY, et al. Adiponutrin functions as a nutritionally regulated lysophosphatidic acid acyltransferase. Cell Metab. 2012;15:691–702.

[20] Yki-Järvinen H. Non-alcoholic fatty liver disease as a cause and a consequence of metabolic syndrome. Lancet Diabetes Endocrinol 2014;2:901–10.

[21] Lallukka S, Sevastianova K, Perttilä J, Hakkarainen A, Orho-Melander M, Lundbom N, et al. Adipose tissue is inflamed in NAFLD due to obesity but not in NAFLD due to genetic variation in PNPLA3. Diabetologia 2013;56:886–92.

[22] Kotronen A, Johansson LE, Johansson LM, Roos C, Westerbacka J, Hamsten A, et al. A common variant in PNPLA3, which encodes adiponutrin, is associated with liver fat content in humans. Diabetologia 2009;52:1056–60.

[23] Alberti KG, Zimmet PZ. Definition, diagnosis and classification of diabetes mellitus and its complications. Part 1: diagnosis and classification of diabetes mellitus provisional report of a WHO consultation. Diabet. Med.

1998;15:539–553.

[24] Matthews DR, Hosker JP, Rudenski AS, Naylor BA, Treacher DF, Turner RC. Homeostasis model assessment: insulin resistance and beta-cell function from fasting plasma glucose and insulin concentrations in man. Diabetologia 1985;28:412–9.

[25] DeFronzo RA, Matsuda M. Reduced time points to calculate the composite index. Diabetes Care. 2010;33:e93–e93.

[26] Brunt EM, Janney CG, Di Bisceglie AM, Neuschwander-Tetri BA, Bacon BR. Nonalcoholic steatohepatitis: a proposal for grading and staging the histological lesions. Am. J. Gastroenterol. 1999;94:2467–2474.

[27] Korenblat KM, Fabbrini E, Mohammed BS, Klein S. Liver, Muscle, and Adipose Tissue Insulin Action Is Directly Related to Intrahepatic Triglyceride Content in Obese Subjects. Gastroenterology 2008;134:1369–75.

[28] Lazo M, Hernaez R, Eberhardt MS, Bonekamp S, Kamel I, Guallar E, et al. Prevalence of nonalcoholic fatty liver disease in the United States: the Third National Health and Nutrition Examination Survey, 1988-1994. Am J Epidemiol 2013;178:38–45.

[29] Donnelly KL, Smith CI, Schwarzenberg SJ, Jessurun J, Boldt MD, Parks EJ. Sources of fatty acids stored in liver and secreted via lipoproteins in patients with nonalcoholic fatty liver disease. J Clin Invest 2005;115:1343–51.

[30] Fabbrini E, Mohammed BS, Magkos F, Korenblat KM, Patterson BW, Klein S. Alterations in adipose tissue and hepatic lipid kinetics in obese men and women with nonalcoholic fatty liver disease. Gastroenterology 2008;134:424–31.

[31] Lomonaco R, Ortiz-Lopez C, Orsak B, Webb A, Hardies J, Darland C, et al.

Effect of adipose tissue insulin resistance on metabolic parameters and liver histology in obese patients with nonalcoholic fatty liver disease. Hepatology. 2012;55:1389–1397.

[32] Kotronen A, Vehkavaara S, Yki-Järvinen H. Increased liver fat, impaired insulin clearance, and hepatic and adipose tissue insulin resistance in type 2 diabetes. Gastroenterology 2008;135:122–30.

[33] Kotronen A, Seppänen-Laakso T, Westerbacka J, Kiviluoto T, Arola J, Ruskeepää A, et al. Comparison of Lipid and Fatty Acid Compositions of the Liver, Subcutaneous and Intra-abdominal Adipose Tissue, and Serum. Obesity. 2010;18:937-944.

[34] Magkos F, Su X, Bradley D, Fabbrini E, Conte C, Eagon JC, et al. Intrahepatic Diacylglycerol Content Is Associated With Hepatic Insulin Resistance in Obese Subjects. Gastroenterology. 2012;142:1444–1446.

[35] Kumashiro N, Erion DM, Zhang D, Kahn M, Beddow SA, Chu X, et al. Cellular mechanism of insulin resistance in nonalcoholic fatty liver disease. Proc. Natl. Acad. Sci. U.S.A. 2011;108:16381–16385.

[36] Shimizu T. Lipid Mediators in Health and Disease: Enzymes and Receptors as Therapeutic Targets for the Regulation of Immunity and Inflammation. Annu Rev Pharmacol Toxicol. 2009;49:123-150.

[37] Puri P, Baillie RA, Wiest MM, Mirshahi F, Choudhury J, Cheung O, et al. A lipidomic analysis of nonalcoholic fatty liver disease. Hepatology 2007;46:1081–90.

[38] Peter A, Kovarova M, Nadalin S, Cermak T, Königsrainer A, Machicao F, et al. PNPLA3 variant I148M is associated with altered hepatic lipid composition in humans. Diabetologia. 2014;57:2103–2107.

[39] Sookoian S, Pirola CJ. Meta-analysis of the influence of I148M variant of patatin-like phospholipase domain containing 3 gene (PNPLA3) on the susceptibility and histological severity of nonalcoholic fatty liver disease. Hepatology 2011;53:1883–94.

[40] Cheon HG, Cho YS. Protection of palmitic acid-mediated lipotoxicity by arachidonic acid via channeling of palmitic acid into triglycerides in C2C12. J Biomed Sci 2014;21:13.

[41] McPherson S, Hardy T, Henderson E, Burt AD, Day CP, Anstee QM. Evidence of NAFLD progression from steatosis to fibrosing-steatohepatitis using paired biopsies: Implications for prognosis and clinical management. J Hepatol 2015;62:1148–55.

[42] Farrell GC, Teoh NC, McCuskey RS. Hepatic Microcirculation in Fatty Liver Disease. The Anatomical Record 2008;291:684–92.

[43] Rotman Y, Koh C, Zmuda JM, Kleiner DE, Liang TJ. The association of genetic variability in patatin like phospholipase domain containing protein 3 (PNPLA3) with histological severity of nonalcoholic fatty liver disease. Hepatology 2010;52:894–903.

[44] Pirazzi C, Valenti L, Motta BM, Pingitore P, Hedfalk K, Mancina RM et al. PNPLA3 has retinyl-palmitate lipase activity in human hepatic stellate cells. Hum. Mol. Genet. 2014;23:4077-4085.

[45] Finkenstedt A, Auer C, Glodny B, Posch U, Steitzer H, Lanzer G, et al. Patatin-like phospholipase domain-containing protein 3 rs738409-G in recipients of liver transplants is a risk factor for graft steatosis. Clin Gastroenterol Hepatol 2013;11:1667–72.

Figure legends

Fig. 1A. BMI (upper left panels), fasting insulin (upper right panels), liver fat (lower left panels) and adiponectin (lower right panels) between 'Low HOMA-IR' vs. 'High HOMA-IR' (panels on the left side of each comparison) and 'PNPLA3148II' vs. PNPLA3148MM/MI' (panels on the right side of each comparison). Data are shown in mean ± SEM for BMI, and in medians and interquartile ranges for other variables. 'ns' $p>0.05$, *$p<0.05$, **$p<0.01$, ***$p<0.001$, ****$p<0.0001$.

Fig. 1B. Plasma glucose and serum insulin during OGTT between 'Low HOMA-IR' vs. 'High HOMA-IR' (panels on the left side of each comparison) and 'PNPLA3148II' vs. 'PNPLA3148MM/MI', panels on the right side of each comparison). Data are in means ± SEM. 'ns' $p>0.05$, *$p<0.05$, **$p<0.01$, ***$p<0.001$, ****$p<0.0001$.

Fig. 2. Absolute concentrations of hepatic TAGs between groups ('High HOMA-IR' vs. 'Low HOMA-IR', panel on the left; 'PNPLA3148MM/MI' vs. 'PNPLA3148II' groups panel on the right). The color code represents the log of the ratio between means of the groups for an individual TAG. The y-axes denote the number of carbons and the x-axes the number of double bonds. The brighter the red color, the greater increase of absolute concentration of the individual TAG in the 'High HOMA-IR' compared to the 'Low HOMA-IR' group or the PNPLA3148MM/MI' compared to the 'PNPLA3148II' group. *$p<0.05$, **$p<0.01$, ***$p<0.001$.

Fig. 3. Absolute concentrations of hepatic FFAs between groups ('High HOMA-IR' vs. 'Low HOMA-IR', panel on the left; 'PNPLA3148MM/MI' vs. 'PNPLA3148II' groups panel on the right). The y-axes denote the total concentration of free fatty acids. The segments in different color in each column represent individual FFAs. 'ns' $p>0.05$, *$p<0.05$.

Fig. 4. Absolute concentrations of hepatic ceramides between groups ('High HOMA-IR' vs. 'Low HOMA-IR', panel on the left; 'PNPLA3148MM/MI' vs. 'PNPLA3148II' groups panel on the right). The top panel represents the structure of a ceramide. In the heatmaps, the color code indicates the log of the ratio between means of the groups for an individual ceramide. The y-axes denote the fatty acyl chain and the x-axes the sphingoid base species. The brighter the red color, the greater increase of absolute concentration of the individual ceramide in the 'High HOMA-IR' compared to the 'Low HOMA-IR' group or the PNPLA3148MM/MI' compared to the 'PNPLA3148II' group. *$p<0.05$, **$p<0.01$, ***$p<0.001$.

Fig. 5. Pathways of ceramide synthesis. The schematic diagram (panel on the left) depicts the pathways of ceramide metabolism (14). Ceramides can be synthesized via the *de novo* synthetic pathway in which palmitate is metabolized to dihydroceramides prior to formation of ceramides (heatmap on the left). They can also be formed via the salvage pathway from hexosylceramides (middle heatmap) and via sphingomyelin hydrolysis (heatmap on the right). Ceramides are degraded by ceramidase, which is upregulated by adiponectin. In the heatmaps, the color code indicates the log of the ratio between means of the 'High' vs. 'Low HOMA-IR' groups for an individual lipid. The y-axes denote the fatty acyl chain and the x-axes the sphingoid base. The brighter the red color, the greater increase of absolute concentration of the individual

lipid. *p<0.05, **p<0.01.

Table

Table 1. Clinical characteristics of the study subjects according to HOMA-IR and the PNPLA3 genotype at rs738409.

Total	Low HOMA-IR (n=63)	High HOMA-IR (n=62)	PNPLA3^{148II} (n=64)	PNPLA3$^{148MM/MI}$ (n=61)
Age (years)	49.2 ± 1.1	46.2 ± 1.1	46.2 ± 1.1	49.3 ± 1.0*
Gender (n, % women)	45 (71.4)	38 (61.3)	45 (70.3)	38 (62.3)
Waist circumference (cm)	127.6 ± 1.8	135.5 ± 1.6**	130.2 ± 1.8	132.9 ± 1.8
fP-Glucose (mmol/l)	5.5 (4.7 - 6.0)	6.1 (5.6 – 6.8)****	5.8 (5.2 - 6.4)	5.7 (5.3 - 6.5)
HbA_{1C} (%)	5.7 (5.5 - 6.1)	6.0 (5.6 - 6.5)	5.7 (5.5 - 6.3)	5.9 (5.5 - 6.3)
HbA_{1C} (mmol/mol)	38.8 (36.6 – 43.2)	42.1 (37.7 – 47.0)	38.8 (36.9 – 45.4)	41.0 (36.9 – 45.1)
HOMA-IR	1.8 (1.3 – 2.7)	4.8 (3.9 – 5.8)****	3.2 (1.9 - 4.5)	3.2 (1.7 - 5.1)
Matsuda ISI	89.8 (65.7 – 141.9)	35.5 (27.3 – 45.1)****	53.7 (35.0 – 87.8)	51.2 (34.3 – 96.8)
fP-Triglycerides (mmol/l)	1.12 (0.91 - 1.66)	1.34 (1.15 - 1.85)*	1.29 (0.97 - 1.80)	1.26 (1.00 - 1.66)
fP-HDL cholesterol (mmol/l)	1.17 (1.00 - 1.44)	1.02 (0.89 - 1.21)**	1.10 (0.95 - 1.36)	1.11 (0.95 - 1.30)
fP-LDL cholesterol (mmol/l)	2.4 ± 0.1	2.5 ± 0.1	2.5 ± 0.1	2.4 ± 0.1
Liver fat (%)	5 (0 - 20)	15 (5 - 33)**	5 (0 - 28)	15 (5 - 30)*
P-AST (IU/l)	30 (25 - 37)	31 (26 - 38)	28 (24 - 33)	32 (26 - 41)**
P-ALT (IU/l)	28 (22 - 40)	38 (30 - 51)****	31 (24 - 45)	36 (27 - 46)
P-ALP (IU/l)	65 ± 2	65 ± 2	66 ± 2	64 ± 2
P-GGT (U/l)	26 (19 - 38)	36 (23 - 52)*	28 (20 - 44)	32 (22 - 52)
P-Albumin (g/l)	37.6 (36.6 - 39.3)	38.0 (36.1 – 39.7)	37.8 (36.3 - 39.4)	37.9 (36.0 - 39.3)
B-Platelets (x10^9/l)	246 ± 9	252 ± 8	258 ± 9	240 ± 7
PNPLA3 (CC/CG/GG) (n)	32/27/4	32/27/3	64/0/0	0/54/7****
Use of statins (n)	18	22	22	18
NASH (%)	11.1	29.0*	12.5	27.9*
Women/men with NASH (n)	4/3	9/9	4/4	9/8

Data are in n (%), means ± SEM or median (25th-75th percentile), as appropriate. *$P \leq 0.05$. **$P \leq 0.01$. ***$P \leq 0.001$. ****$P \leq 0.0001$.

Figure 1

Click here to download high resolution image

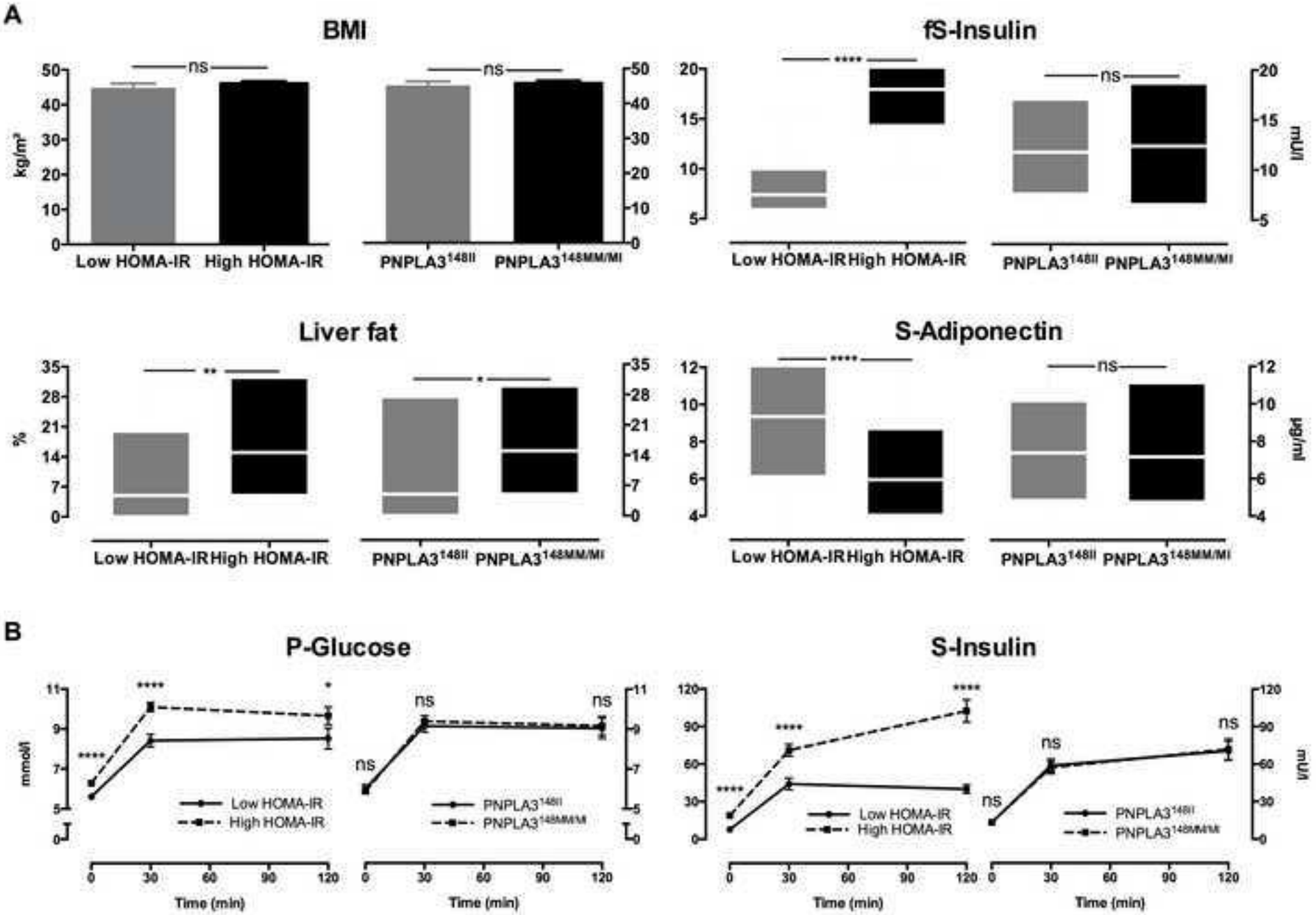

Figure 2

Click here to download high resolution image

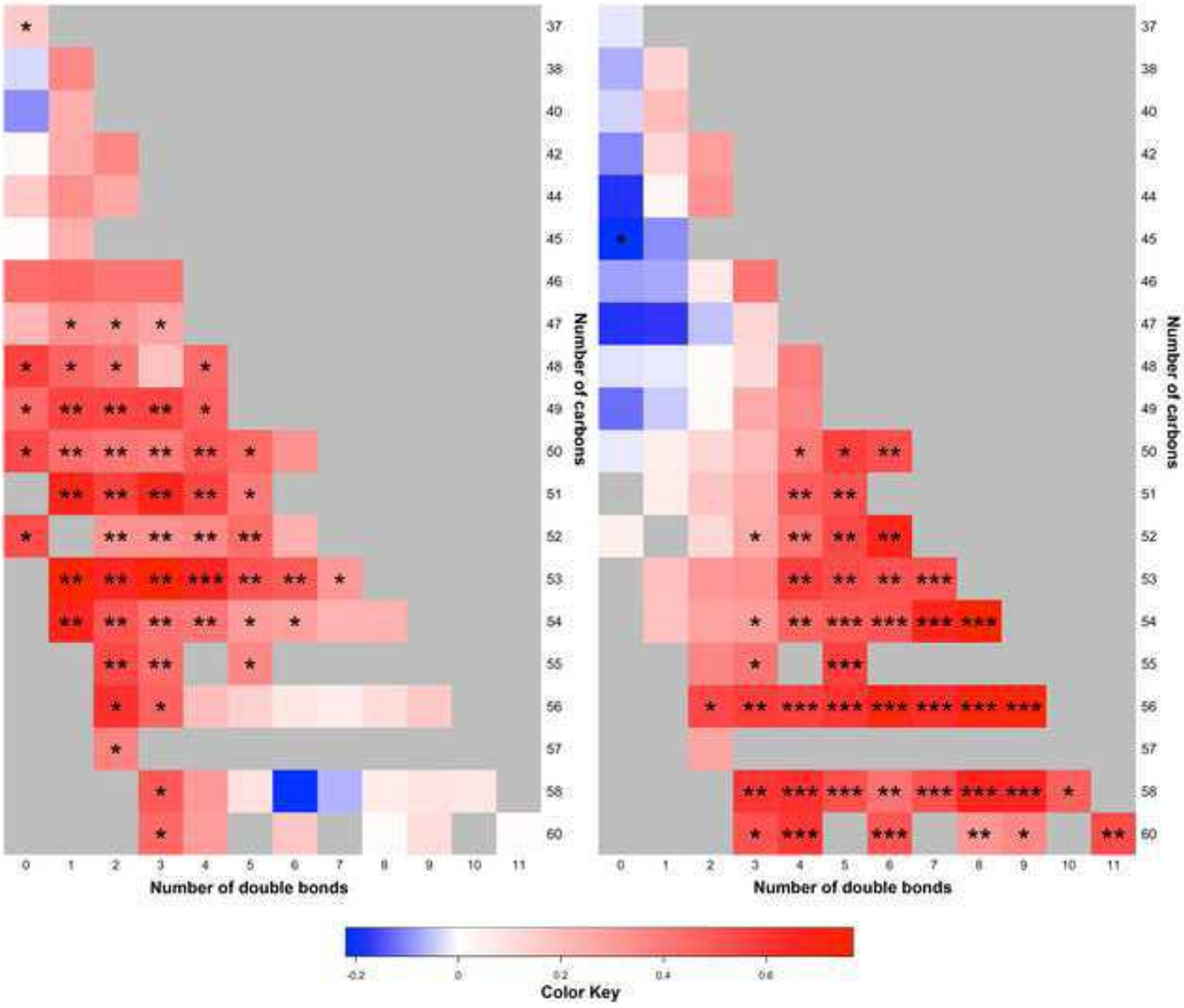

Figure 3

Click here to download high resolution image

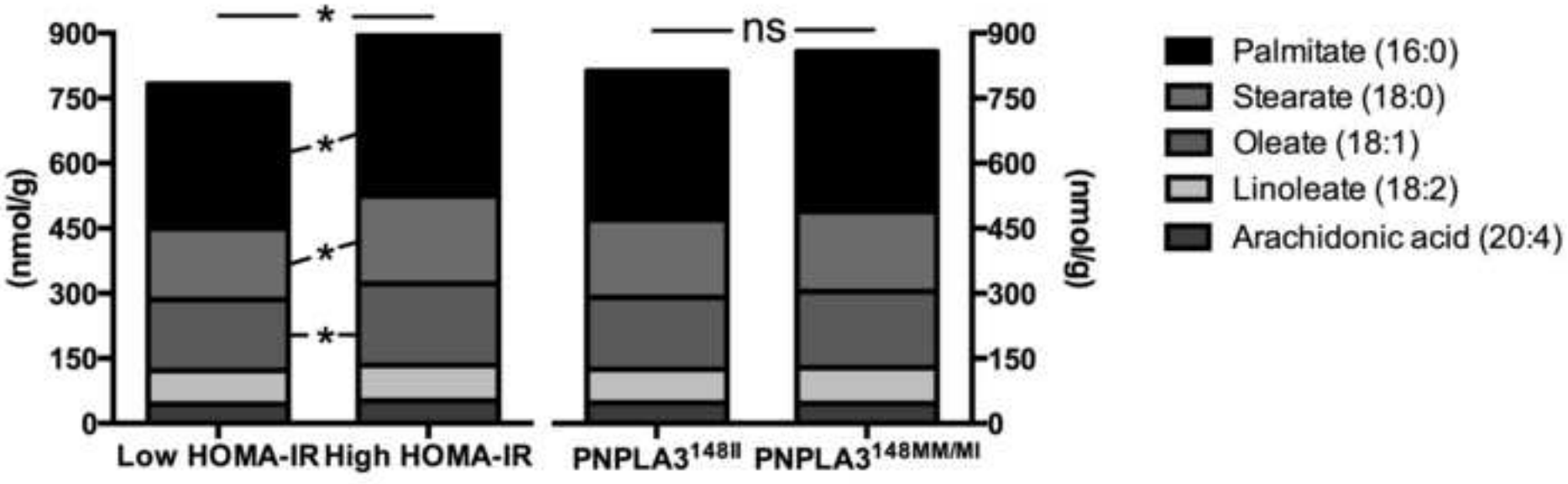

Figure 4

Click here to download high resolution image

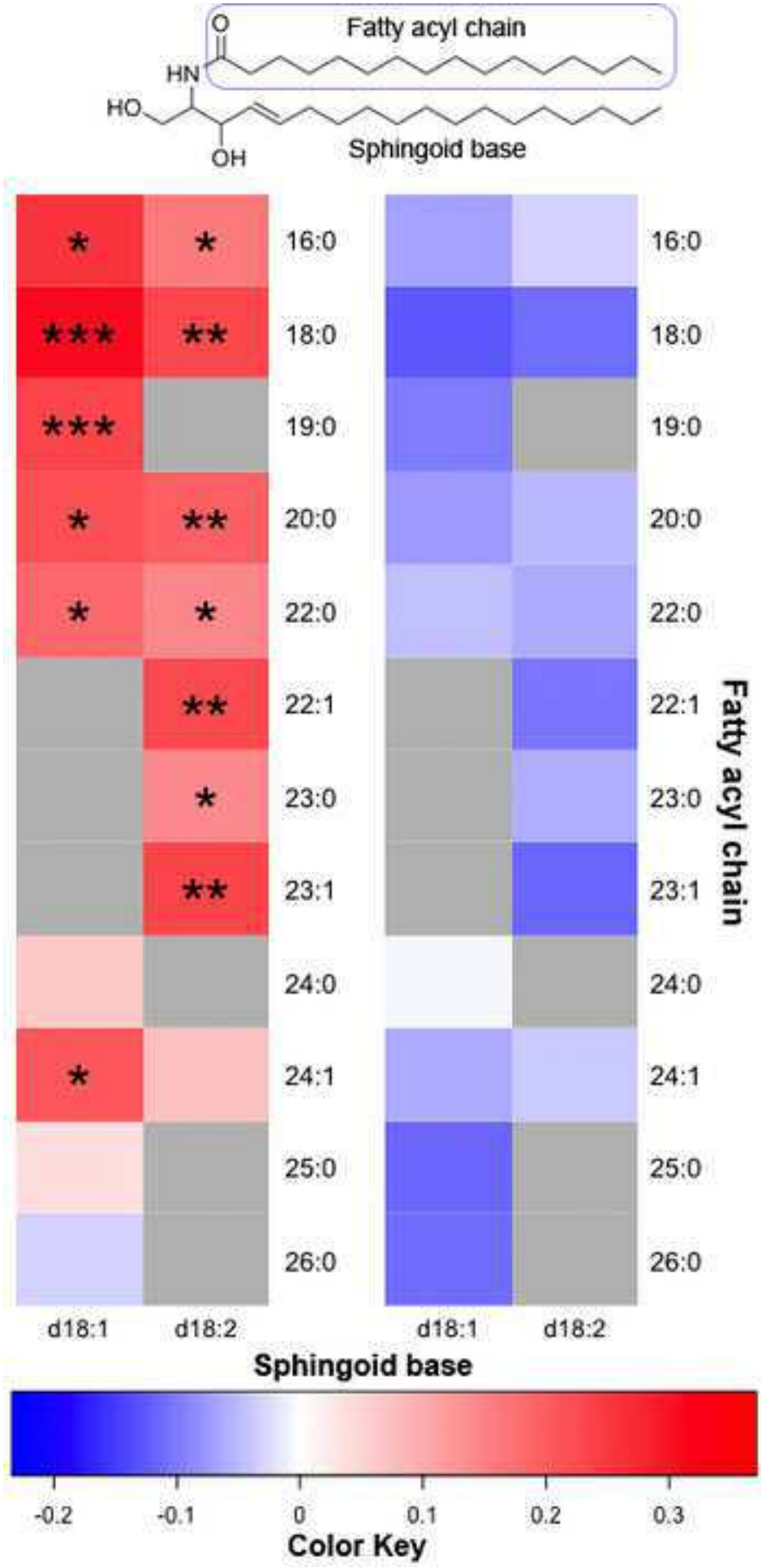

Figure 5

Click here to download high resolution image

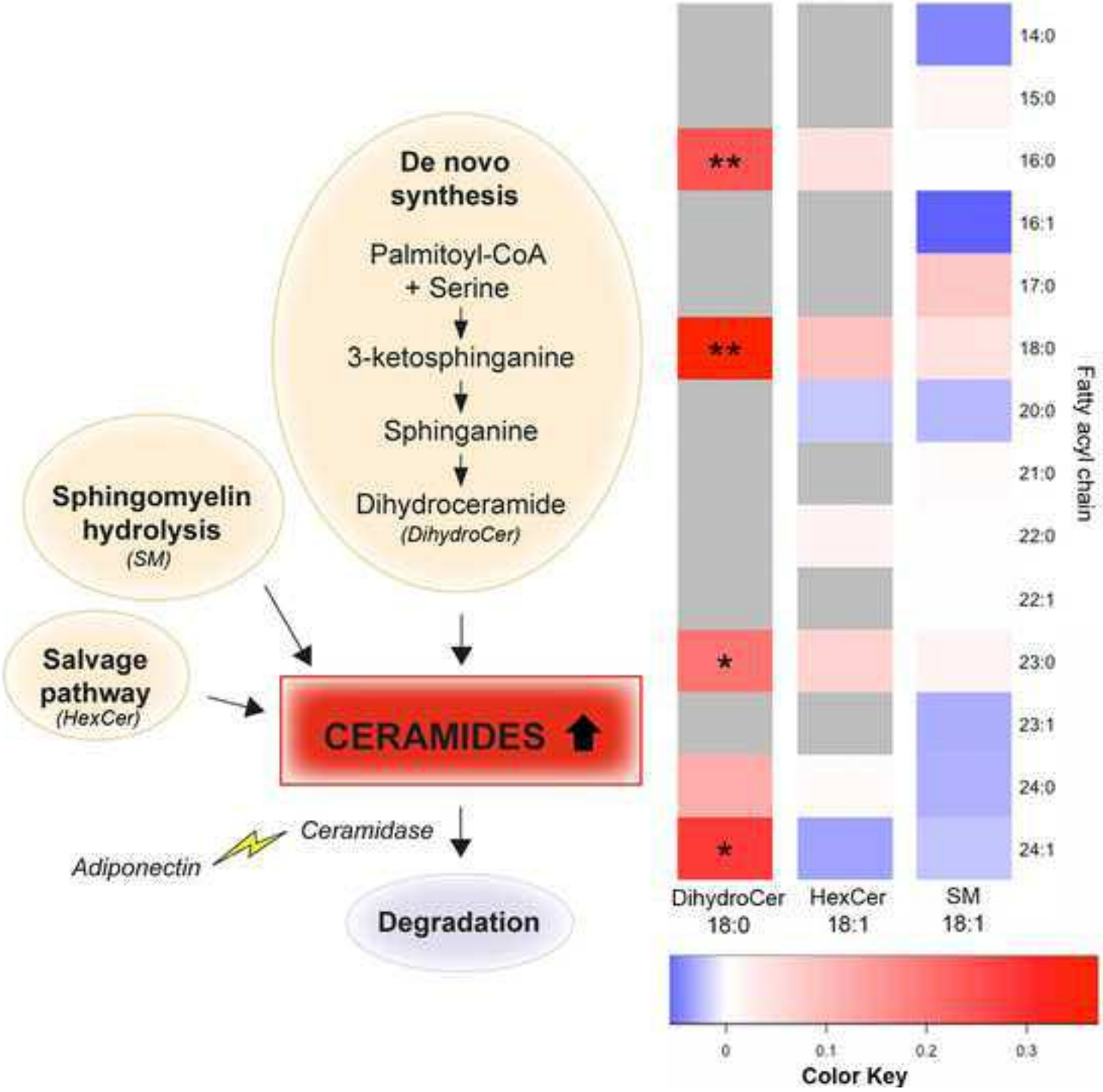

Supplementary material

Click here to download Supplementary material: Supplementary_material_051115_FINAL.docx